Fluid Phase Equilibria 414 (2016) 93–100

Contents lists available at ScienceDirect

Fluid Phase Equilibria

journal homepage: www.elsevier.com/locate/fluid

Interactions of pyridinium, pyrrolidinium or piperidinium based ionic liquids with water: Measurements and COSMO-RS modelling

Imran Khan [a], Mohamed Taha [a], Simão P. Pinho [b], João A.P. Coutinho [a, *]

[a] CICECO – Aveiro Departamento de Química, Universidade de Aveiro, 3810-193, Aveiro, Portugal
[b] Associate Laboratory LSRE/LCM, Departamento de Tecnologia Química e Biológica, Instituto Politécnico de Bragança, Campus de Santa Apolónia, 5301-857, Bragança, Portugal

ARTICLE INFO

Article history:
Received 23 October 2015
Received in revised form
6 January 2016
Accepted 8 January 2016
Available online 12 January 2016

Keywords:
Activity coefficient
Water activity
COSMO-RS
Hydrogen bonding
Excess enthalpy

ABSTRACT

Looking for a better knowledge concerning water and ionic liquids (ILs) interactions, a systematic study of the activity coefficients of water in pyridinium, pyrrolidinium and piperidinium-based ILs at 298.2 K is here presented based on water activity measurements. Additionally, the study of the structural effects of the pyridinium-based cation is also pursued. The results show that non-aromatic ILs are interacting more with water than aromatic ones, and among the ortho, meta and para isomers of 1-butyl-methylpyridinium chloride, the ortho position confers a more hydrophilic character to that specific IL. The physical-chemistry of the solutions was interpreted based on dissociation constants, natural bond orbitals and excess enthalpies providing a sound basis for the interpretation of the experimental observations. These results show that hydrogen bonding controls the behavior of these systems, being the anion-water one of the most relevant interactions, but modulated by the anion–cation interactions.

1. Introduction

Ionic liquids (ILs) are organic salts, usually consisting of a large organic cation and an organic or inorganic anion, which are liquid at temperatures below 100 °C. ILs have been proposed as novel green solvents because they have been considered environmentally friendly and applicable in the development of green technologies [1,2]. The unique characteristics of ILs make them suitable alternatives to classical organic solvents and as such, they have been applied in various fields like electrochemistry, liquid phase extraction, catalysis for clean technology, and polymerization processes [3–6]. Recently a review on energy applications of ILs revealed wider fields of interest of ILs [7].

While the focus of most works dealing with ILs have been the imidazolium based ILs, other cyclic, aromatic or non-aromatic cations may also be relevant and contribute to the design of ILs with better performance. Despite pyridinium-based ILs present larger viscosities than their equivalent imidazolium compounds, they possess some interesting properties such as bactericidal and fungicidal effects [8], corrosion inhibition efficiency [9], ability to interact with peptides [10] and low ecotoxicity [11–13]. They have been proposed for many potential applications such as fuel desulfurization [14], extraction [15,16], catalysis [17,18], CO_2 capture [19–21] and cellulose dissolution [22,23]. Moreover, the low cost of pyridine in comparison to methylimidazole further drives the research of applications based on the former cation. Pyrrolidinium based ILs showed higher selectivity in the separation of aromatic from aliphatic hydrocarbons, [24–26] and also for the extraction of sulfur compounds from hydrocarbons mixtures [26,27]. Among the studied ILs, piperidinium and pyrrolidinium ILs exhibit lower viscosities and higher cathodic stabilities, consequently attractive in the field of electrochemistry [28–31]. Piperidinium and pyridinium have also been used in the extraction of the metal ions [17,18]. A comparative study of piperidinium and imidazolium based ILs was briefly discussed by Shukla and Saha [32]. Recently, Neumann [33] studied the biodegradability of pyrrolidinium, piperidinium, and pyridinium-based ILs suggesting some rules for the structural design of ILs with a reduced environmental hazard. The interest in these salts is thus based not only on basic science purposes, but has also been driven by practical applications.

Addition of water can change significantly ILs properties such as viscosity [34], density [34], surface tension [35], electrical conductivity [36–38], and reactivity [39,40] as well as solvation and solubility properties [41,42]. In general ILs with highly delocalized charged anions such as PF_6^- and Tf_2N^- are hydrophobic in nature,

* Corresponding author.
E-mail address: jcoutinho@ua.pt (J.A.P. Coutinho).

http://dx.doi.org/10.1016/j.fluid.2016.01.014
0378-3812/

and ILs with halide anions such as Cl^- or Br^-, phosphate ($R_2PO_4^-$), carboxylate (COO^-) are hydrophilic in nature. Anouti et al. [43] studied aggregation behavior of pyrrolidinium alkycarboxylates protic IL as potential new surfactants in aqueous media. Latter, Anouti et al. [44] studied the interaction of some pyrrolidinium carboxylate PILs ([Pyrr][$C_nH_{2n+1}COO$]) with water, and showed higher ability to aggregate in water, even for the shortest alkyl-chain length (n = 5). Experimental and theoretical studies of piperidinium based ILs in water showed the capabilities of liquid–liquid extraction of aromatic or sulfur compounds [45]. The effect of water on ILs are much better studied on imidazolium based ILs [38,46–48] and studies on pyridinium, pyrrolidinium and piperidinium aqueous solutions are very scarce [49–51]. Generally, these studies show that water interaction with ILs is mostly influenced by the anion and, to a lesser extent, by the cation [52–55], but the cation effect has been poorly explored.

COSMO-RS (COSMO for Real Solvents), a quantum chemical-based thermodynamic prediction model has been used to study the interactions between water and ILs [48]. The main advantage of COSMO-RS [56,57], compared to widely used excess Gibbs free energy models [58,59], is that it does not require any experimental data to predict phase equilibria or molecular interactions. Recently, Khan et al. [48,60] showed that model is not able to predict water activity coefficients in water-IL systems with the desired accuracy, but qualitative trends can be explained and interpreted using this approach.

The water activity coefficients of the systems here studied were obtained from water activity measurements in six binary water + ILs mixtures based on pyridinium, pyrrolidinium or piperidinium cations, maintaining chloride as the anion. To deepen the understanding of water-ILs mixtures at the molecular level, and understand the water-IL interactions, COSMO-RS was evaluated by comparing its predictions against the experimental data. Finally that model was used to estimate the energetic effects in those systems.

2. Experimental section

2.1. Materials

The studied ILs 1-butylpyridinium chloride, [C_4py]Cl (98 wt%); 1-butyl-2-methylpyridinium chloride, *o*-[C_4mpy]Cl (99 wt%); 1-butyl-3-methylpyridinium chloride, *m*-[C_4mpy]Cl (99 wt%); 1-butyl-4-methylpyridinium chloride, *p*-[C_4mpy]Cl (98 wt%); 1-butyl-1-methylpyrrolidinium chloride, [C_4mpyr]Cl (98 wt%) and 1-butyl-1-methylpiperidinium chloride, [C_4mpip]Cl (99 wt%) were obtained from IoLiTec (Germany). Fig. 1 depicts the chemical structures of the studied of pyridinium, pyrrolidinium or piperidinium-based ILs. To eliminate water and other volatile compounds, each IL was previously dried at a temperature close to 323 K and at high vacuum ($\approx 10^{-3}$ Pa), under constant stirring, for a minimum period of 48 h. The purities of these ILs were further checked by ^{1}H, and ^{13}C and were shown to be ≥99 wt %. The water content of each ionic liquid was determined by Karl Fischer titration [48], and found to be less than 30×10^{-6} mass fraction. Double distilled and purified water was used in all experiments.

2.2. Measurement of water activities and activity coefficients

The measurements of water activities (a_w) were performed using a Novasina hygrometer LabMaster-a_w (Switzerland). The detailed description of the water activity measurement is given elsewhere [48]. The accuracy of the instrument is 0.001 a_w attained under controlled chamber temperature conditions (±0.15 K). To attain that accuracy, a calibration using aqueous LiCl solutions at selected salt molalities was implemented, comparing to the data compiled by Hamer and Wu [61]. The weight measurement for each sample was found to give an uncertainty of 0.0001 in water mole fraction. The water activity coefficient (γ_w) is obtained by

$$\gamma_w = \frac{a_w}{x_w} \tag{1}$$

where x_w is the water mole fraction.

2.3. COSMO-RS modeling

The COSMO-RS model is a very progressive kind of a dielectric model, where molecules are placed in a conductor as the reference state. The description of COSMO-RS features can be found elsewhere [56]. The most fundamental concept of COSMO-RS is to calculate the interaction energy between species using polarization charge densities i.e. σ and σ′. The sum of electrostatic misfit (E_{MF}), hydrogen bond (E_{HB}), and van der Waals interaction energies (E_{VdW}) gives the total molecular interaction energy [62]. Each specific interaction can be predicted in terms of σ and σ′ of the contacting surfaces with the equation given below:

$$E_{MF}(\sigma,\sigma') = a_{\text{eff}}\frac{\alpha'}{2}(\sigma+\sigma')^2 \tag{2}$$

$$E_{\text{HB}} = a_{\text{eff}}c_{hb}min\left(0,\ \sigma\sigma' + \sigma_{hb}^2\right) \tag{3}$$

$$E_{\text{VdW}} = a_{\text{eff}}\left(\tau_{vdW} + \tau'_{vdW}\right) \tag{4}$$

where, a_{eff} is the size of a thermodynamically independent contact area (effective area), α' is an adjustable parameter, c_{hb} is the strength coefficient, σ_{hb} is the polarization charge density threshold for hydrogen bond, and τ_{vdW} is the element-specific parameter for dispersion coefficient. The surface charge densities information are used in the COSMO-RS framework to obtain the σ-profile and σ-potentials, which gives valuable information in terms of properties and interaction behavior of the compound [62,63]. The chemical potential of segment having σ charge density (in the ensemble S) is given by Equation 5 [63]. Lower value of μ(σ) at a particular σ represents better affinity for that polarity and vice versa.

$$\mu_s(\sigma) = -RT\ ln\left[\int d\sigma' p_s(\sigma)\exp\left\{-\frac{1}{2}\alpha'^{(\alpha+\alpha')^2} - \mu'_s(\sigma')\Big/RT\right\}\right] \tag{5}$$

where R is the ideal gas constant and T is the absolute temperature. The procedure to predict the activity coefficient by COSMO-RS can be found elsewhere [64,65], as well as the methodology to calculate the excess enthalpy [66]. For that purposes, COSMOtherm software using the parameter file BP_TZVP_C30_1401 (COSMOlogic GmbH & Co KG, Leverkusen, Germany) [67] was used.

2.4. Dissociation constant

Dissociation constant ($K_{d(IL)}$) of the IL can give a good contribution for understanding the ILs ions–water interactions. The ($K_{d(IL)}$) of an IL, at infinite dilution in water, is obtained from the Gibbs free energy ($\Delta G_{d(IL)}$) of the dissociation equilibrium as calculated by COSMOtherm,

$$[C-A] \leftrightarrow C^+ + A^- \tag{6}$$

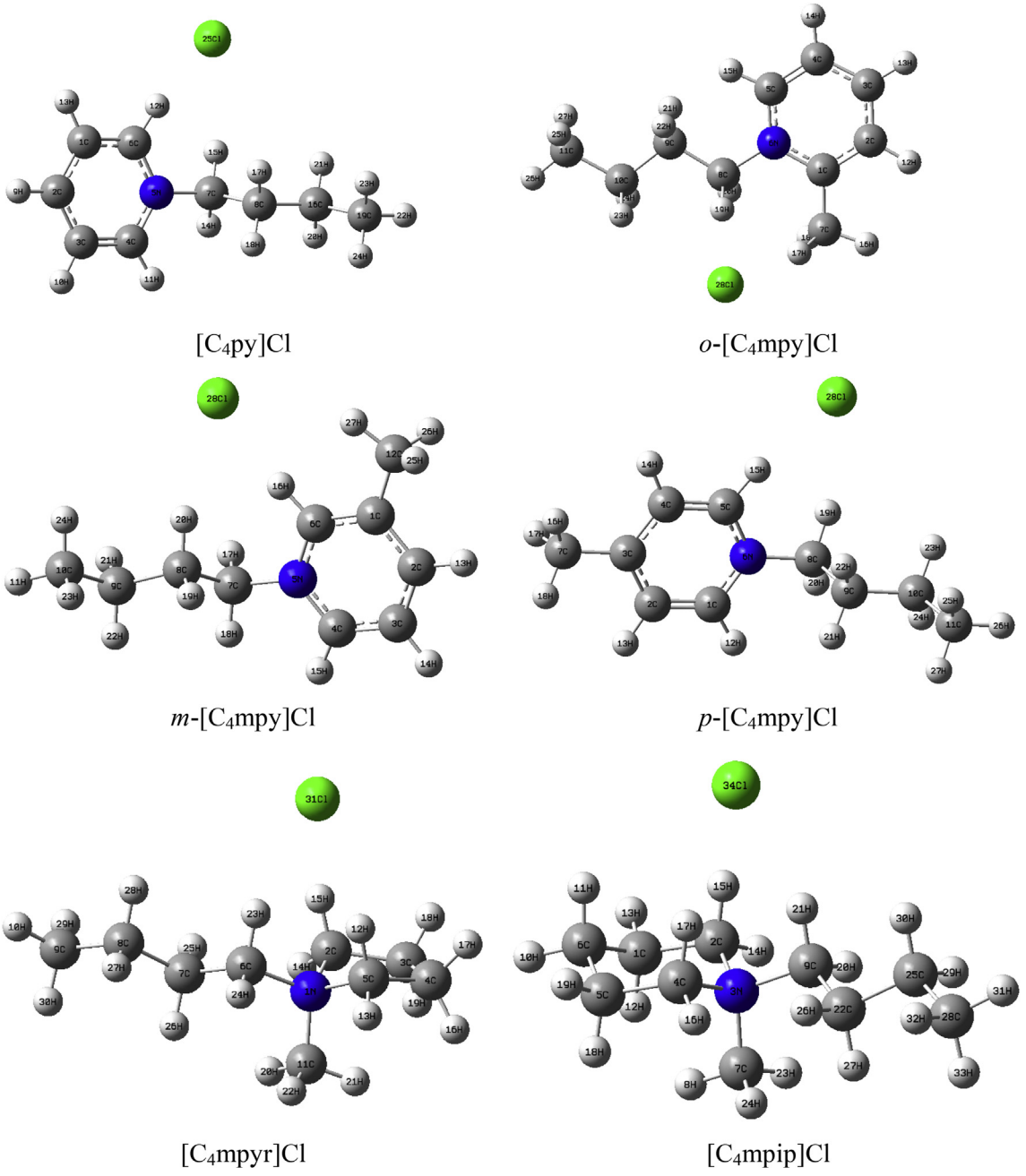

Fig. 1. Structures of investigated ILs, showing the optimized geometries of the ion-pairs for the lowest energy at the DFT/TZVP levels (as given in Section 2.4).

where [C−A], C^+, and A^- refers to the ion-pair, cation, and anion of an IL, respectively. To generate the σ-profile of the ion-pairs ([C−A]), their geometries were optimized using DFT-RI/b-p/TZVP method in gas phase and COSMO model. An initial guess structure for the ([C−A]) was generated by locating the anion (Cl^-) with the most positive areas of the cation. Vibrational frequencies were done to confirm that all the optimized ion-pairs are true minima, and the optimized ion-pairs are shown in Fig. 1.

The $\Delta G_{d(IL)}$ of the dissociation process is difference in the total Gibbs energies between the isolated IL's ions and the ion-pair.

$$\Delta G_{d(IL)} = (G_{C^+} + G_{A^-}) - G_{[C-A]} \quad (7)$$

The values for G_{C^+}, G_{A^-}, and $G_{[C-A]}$ are calculated from the DFT gas phase energies ($E_{i,DFT}$) and the free energy of solvation ($\Delta G_{i,solv}$) as computed by COSMOtherm,

$$G_i = E_{i,\,DFT} + \Delta G_{i,solv} \quad (8)$$

The $K_{d(IL)}$ is calculated by,

$$K_{d(IL)} = \exp\left(-\Delta G_{d(IL)} \Big/ RT\right) \quad (9)$$

3. Results and discussions

The measured water activity coefficients in the pyridinium, pyrrolidinium and piperidinium-based ILs at 298.2 K are given in Table 1. To the best of our knowledge no data was published before

for these ILs, at this temperature or concentration range. The choice of several pyridinium, pyrrolidinium or piperidinium based ILs as cation, and chloride as common anion, aims at understanding the molecular interactions between water and ILs, but also to study the structural effects of the pyridinium-based cation on the mixing of water in the miscibility region. Fig. 2 presents the behavior of the different studied systems, showing significant effect of ILs in water. All the studied system shows activity coefficient lower than one showing a favorable interaction between water and ILs, according to the following increasing rank:

$$[C_4mim]Cl[48] < [C_4py]Cl < p-[C_4mpy]Cl \cong m-[C_4mpy]Cl < o-[C_4mpy]Cl < [C_4mpy]Cl < [C_4mpip]Cl < [C_4mpyr]Cl$$

Very often the anion is used to control the water miscibility, but the cation can also influence the hydrophobicity [68–70] or hydrogen bonding ability. On visualizing the interaction trend it is very clear that non-aromatic based ILs ([C_4mpyr]Cl, [C_4mpip]Cl) shows stronger interactions than the aromatic based ILs (*p*-[C_4mpy]Cl, *m*-[C_4mpy]Cl, [C_4py]Cl, *o*-[C_4mpy]Cl). Further, unforeseen behavior was observed in the case of (*o*, *m*, or *p*)-[C_4mpy]Cl and [C_4py]Cl. It was expected that (*o*, *m*, or *p*)-[C_4mpy]Cl would show lesser interaction with water due to extra methyl group attached, but the interaction are identical or even superior in the case of *o*-[C_4mpy]Cl. The ranking of interaction of the studied ILs with water based on the COSMO-RS model follows the same order [C_4mim]Cl < [C_4py]Cl < *p*-[C_4mpy]Cl ≅ *m*-[C_4mpy]Cl < *o*-[C_4mpy]Cl < [C_4mpip]Cl < [C_4mpyr]Cl, excepting [C_4mim]Cl in the very diluted region. In that region, [C_4mim]Cl is interacting slightly more than other studied ILs, but for higher IL concentrations the interaction decreases in agreement to the predictions by the COSMO-RS model. Differences in the interaction behavior of imidazolium or pyridinium based ILs with water can be explained considering that pyridinium based IL form a strong anion–HOH–anion complex, along with the H-bonds with the aromatic of the C–H on the pyridinium cation, whereas the imidazolium based ILs present strong anion–cation interactions and steric hindrance from the alkyls, which prevent water molecules from H-bonding with the aromatic C–H other than with the anion [71]. A point deserving also attention in Fig. 2 is that for the series of very similar ionic liquids studied

Table 1
Measured water activity coefficients in the ionic liquids studied at 298.2 K.

H_2O + [C_4py]Cl		H_2O + *o*-[C_4mpy]Cl		H_2O + *m*-[C_4mpy]Cl	
x_{H2O}	γ_{H2O}	x_{H2O}	γ_{H2O}	x_{H2O}	γ_{H2O}
0.9887	1.000	0.9895	0.999	0.9893	0.999
0.9736	0.988	0.9767	0.991	0.9765	0.992
0.9597	0.966	0.9611	0.965	0.9608	0.967
0.9434	0.942	0.9414	0.935	0.9426	0.939
0.9091	0.870	0.9130	0.867	0.9166	0.892
0.8782	0.801	0.8768	0.784	0.8827	0.811
0.8286	0.674	0.8193	0.616	0.8254	0.656
0.7593	0.488	0.7343	0.405	0.7510	0.456
				0.6214	0.224
H_2O + *p*-[C_4mpy]Cl		H_2O + [C_4mpyr]Cl		H_2O + [C_4mpip]Cl	
x_{H2O}	γ_{H2O}	x_{H2O}	γ_{H2O}	x_{H2O}	γ_{H2O}
0.9892	0.998	0.9894	0.997	0.9899	0.999
0.9769	0.990	0.9781	0.989	0.9776	0.991
0.9603	0.967	0.9603	0.954	0.9622	0.969
0.9413	0.937	0.9463	0.921	0.9432	0.932
0.9119	0.883	0.9261	0.857	0.9196	0.874
0.8763	0.793	0.8984	0.739	0.8843	0.781
0.8170	0.631	0.8588	0.576	0.8231	0.573
0.7391	0.426	0.8040	0.392	0.7469	0.404
0.6781	0.327	0.7554	0.264		

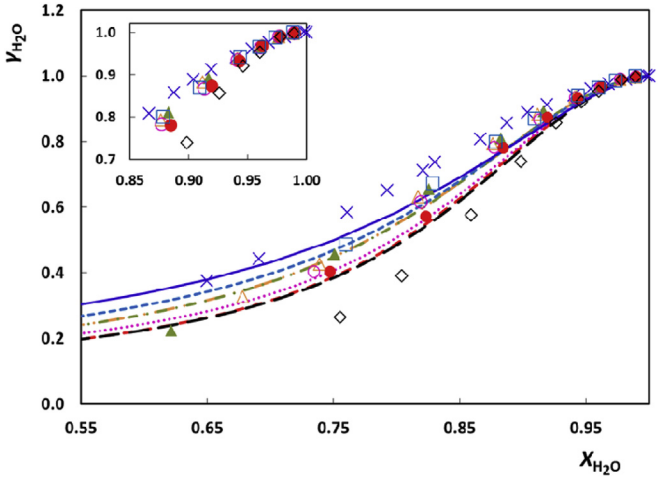

Fig. 2. Activity coefficient of water (γH_2O) versus water mole fraction at 298.2 K, for the [C_4py]Cl (□, square dot line), o-[C_4mpy]Cl (○, round dot line), m-[C_4mpy]Cl (▲, dash dot line), p-[C_4mpy]Cl (△, long dash dot dot line), [C_4mpyr]Cl (◊, long dash line), [C_4mpip]Cl (●, dash line), [C_4mim]Cl [48] (×, solid line). The symbols and lines indicate the experimental and COSMO-RS predictions, respectively.

in this work, COSMO-RS predicts the activity coefficients in a much closer range than the experimental data. However, if looking for studies about the influence of the anion on the water activity in mixtures containing choline based ionic liquids [72], the predicted curves are, on the contrary, wider than the experimental results. Even if there is room for improvements, in both cases very coherent qualitatively results were observed looking to the predicted curves, when compared to the experimental ranking.

The $\Delta G_{d(IL)}$ and $K_{d(IL)}$ values of the dissociation process of the ILs are reported in Table 2, and the values of the ΔG_{solv} are summarized in Table S1 (supporting material). Table S1 shows that absolute ΔG_{solv} values of the ILs ions are higher than those of the corresponding ILs, suggesting that the hydration of the ILs ions is the driving force of the dissociation processes. The degree of the dissociation can be seen from the $pK_{d(IL)}$ values (Table 2), the lower the $pK_{d(IL)}$ value, the higher is its tendency to dissociate. The $pK_{d(IL)}$ values of the studied ILs range from ~3.1 to ~4.1, and thus they are not completely dissociated in water. The $K_{d(IL)}$ values of the ILs were found to follow the order: [C_4mpip]Cl > [C_4mpyr]Cl > *o*-[C_4mpy]Cl > [C_4py]Cl ≅ *m*-[C_4mpy]Cl ≅ *p*-[C_4mpy]Cl > [C_4mim]Cl. Interestingly, this order reflects the rank based on the water activity coefficients, except for [C_4mpip]Cl and [C_4mpyr]Cl which are reversed. The ion–pair interaction in [C_4mpyr]Cl is stronger than that of [C_4mpip]Cl, but its smaller molar volume favors a higher interaction with water. The $pK_{d(IL)}$ values reveal that the aromatic ILs present greater cation–anion interactions than the non-aromatic ILs. Moreover, the cation–anion interaction of *o*-[C_4mpy]Cl is smaller than the other aromatic ILs, consistent with

Table 2
Calculated free energies (kcal mol^{-1}), and dissociation constants of the ILs in water at 298.15 K.

Ionic liquids	$\Delta G_{d(IL)}$	$K_{d(IL)}$	$pK_{d(IL)}$
[C_4mpyr]Cl	4.59	4.32×10^{-04}	3.36
[C_4mpip]Cl	4.27	7.44×10^{-04}	3.13
[C_4py]Cl	4.84	2.85×10^{-04}	3.54
o-[C_4mpy]Cl	4.65	3.90×10^{-04}	3.41
m-[C_4mpy]Cl	4.86	2.73×10^{-04}	3.56
p-[C_4mpy]Cl	4.87	2.71×10^{-04}	3.57
[C_4mim]Cl	5.60	7.85×10^{-05}	4.10

the indications from the water activity coefficients.

To gain more insight into the cation–anion interactions, natural bond orbital (NBO) analysis was performed at the B3LYP/DGTZV level of theory using the Gaussian 09 package [73]. NBO analysis is in this case useful for investigating the charge-delocalization between the lone pairs of Cl^- and the ring moiety of the IL cations by applying second order perturbation theory. For each donor orbital (i) and acceptor (j), the stabilization energy E^2 associated with electron delocalization between both orbitals is defined as,

$$E^2 = q_i \frac{F(i,j)^2}{\varepsilon_i - \varepsilon_j}, \tag{10}$$

where q_i refers to the ith donor orbital occupancy, $F(i,j)^2$ is the off-diagonal elements associated with the NBO Kohn–Sham Matrix, and (ε_i and ε_j) are the diagonal elements (orbital energies).

The larger E^2 value represents the higher interaction between electron donors and acceptors, which means that greater extent of charge-transfer between electron donors and acceptor orbitals. Table S2 lists the E^2 values for the cation–anion interactions. The strongest delocalization in [C_4py]Cl and [C_4mim]Cl involve the interactions of the chloride anion lone pairs with the C–H antibonding, $n_{(4)Cl} \rightarrow \sigma^*_{C6-H12}$ (6.74 kcal/mol) and $n_{(4)Cl} \rightarrow \sigma^*_{C1-H5}$ (8.13 kcal/mol), respectively. The strong interaction between the Cl^- lone pairs and the neighbors antibonding orbitals of the pyridinium cations of *o*-[C_4mpy]Cl, *m*-[C_4mpy]Cl, and p-[C_4mpy]Cl, are $n_{(4)Cl} \rightarrow \sigma^*_{C8-H19}$ (4.26 kcal/mol), $n_{(4)Cl} \rightarrow \sigma^*_{C6-H16}$ (5.90 kcal/mol), and $n_{(4)Cl} \rightarrow \sigma^*_{C5-H15}$ (6.54 kcal/mol), respectively. While the predominant stabilizing interactions found in [C_4mpyr]Cl and [C_4mpip]Cl are $n_{(4)Cl} \rightarrow \sigma^*_{C6-H23}$ (2.87 kcal/mol) and $n_{(4)Cl} \rightarrow \sigma^*_{C9-H21}$(2.73 kcal/mol), respectively. Thus, it can be observed that the values of stabilization energies E^2 for the aromatic ILs are greater than those for the non-aromatic ILs, and the E^2 values for *o*-[C_4mpy]Cl are lower than the other aromatic ILs. The results are in total accordance with the $pK_{d(IL)}$ values and activity coefficients as well. The different sets of results support the notion that the IL interaction with water can be enhanced by minimizing the cation–anion interaction, instead of trying to maximize both cation and the anion interactions with water as proposed by Kurnia et al. [74].

COSMO-RS provides information about molecular interaction, which can be seen from σ-profile and σ-potential, depicted in Fig. 3 and Fig. S1 (supporting material) respectively. Important features concerning water have already been explored by us [48], while considering ions σ-profile and potentials it is interesting to observe that cations [C_4mpip]$^+$, [C_4mpyr]$^+$ and *o*-[C_4mpy]$^+$ are those showing lower hydrogen bond character, suggesting a weaker interaction with the chloride anion, which has a strong hydrogen bond acceptor, validating again the physical-chemical interpretation proposed so far for the binary systems under study, and the experimental trends concerning the water activity coefficient data.

The capability of COSMO-RS as a good semi-quantitative predictive model for activity coefficient was demonstrated before [48], which open an opportunity for us to also predict excess enthalpy (H^E_m) of water and ILs mixtures. The H^E_m is the change in enthalpy upon mixture of the two components and its calculation, in the COSMO-RS, considers the sum of the electrostatic/misfit, $H^E_{m,MF}$; hydrogen bonds, $H^E_{m,HB}$; and van der Waals forces, $H^E_{m,VdW}$ contributions as given below,

$$H^E_m = H^E_{m,MF} + H^E_{m,HB} + H^E_{m,VdW} \tag{11}$$

The mixing of water and studied ILs shows negative H^E_m as predicted by COSMO-RS at 298.2 K, indicating favorable energetic interactions. It can be clearly seen in Fig. 4 that hydrogen bonding

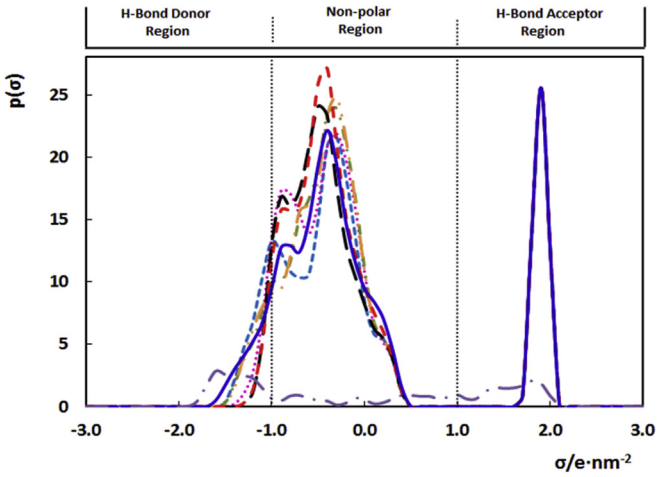

Fig. 3. σ-Profile of H_2O (long dash dot line), [C_4py]Cl (square dot line), o-[C_4mpy]Cl (round dot line), m-[C_4mpy]Cl (dash dot line), p-[C_4mpy]Cl (long dash dot dot line), [C_4mpyr]Cl (long dash line), [C_4mpip]Cl (dash line), [C_4mim]Cl (solid line).

presents higher magnitudes than the other two components to the total excess enthalpy, contributing largely to the exothermicity of the mixtures. Therefore, it confirms that hydrogen bonding is the dominant interaction in these water-IL systems [72,75,76].

Each of these contributions can be estimated by COSMO-RS over all the composition range as depicted in Fig. S2, in the supplementary material. It is worth notice that among isomers *o*-[C_4mpy]Cl deviates clearly from *m*-[C_4mpy]Cl and p-[C_4mpy]Cl curves concerning the electrostatic/misfit and hydrogen bonding contributions to excess enthalpy. Most notably, the trend on hydrogen bonding of *o*-[C_4mpy]Cl is much closer to [C_4mpyr]Cl and [C_4mpip]Cl ILs than to its isomers. The electrostatic interactions (misfit) are attractive, with a small contribution to the total excess enthalpy, whereas van der Waals is the smallest. The H^E_{MF} component suggests that water diminishes the electrostatic interaction between the ions of the ILs, firstly breaking water and [Cation]-[Anion] hydrogen bonds, latter forming of new hydrogen bond network from H_2O-[Cation] and H_2O-[Anion] interactions.

The G^E_m and H^E_m plots (Fig. S3, supporting material) show a minima at x_{H_2O} ~0.75, indicating the formation of a complex between three molecules of water and one molecule of pyridinium/ pyrrolidinium/ or piperidinium ILs, which is also in agreement to the literature [46,75]. The ranking of interaction based on H^E_m from COSMO-RS is [C_4py]Cl < *p*-[C_4mpy]Cl ≅ *m*-[C_4mpy]Cl < *o*-[C_4mpy]Cl < [C_4mpyr]Cl < [C_4mpip]Cl. Very interestingly the H^E_m follows the same order of interaction observed for the experimental activity coefficient except for [C_4mpyr]Cl < [C_4mpip]Cl, which can be connected to the ion–pair interaction as discussed.

Interaction (or binding) energy provides information about the distance between the ion pair. On other hand, the contact probability gives an idea of compactness of the ion pair. Usually, interaction energy and the distance within the ions are inversely proportional, showing dominance of charge–charge interaction in ILs [77]. Fig. 5 shows the contact probability of the entities present in the system with each other. The sum of [Cation]-[Anion] and [Anion]-[Cation] contact probability (Fig. S4) in the studied system follows the trend [C_4mim]Cl > [C_4py]Cl > *p*-[C_4mpy]Cl ≅ *m*-[C_4mpy]Cl > *o*-[C_4mpy]Cl > [C_4mpyr]Cl > [C_4mpip]Cl indicating the cation influence on the hydrophobicity and confirming that the [Cation]-[Anion] interaction plays a role in the behavior of the studied systems [52,68–70]. This rank follows again the behavior shown by the water activity coefficients. A striking feature in Fig. 5

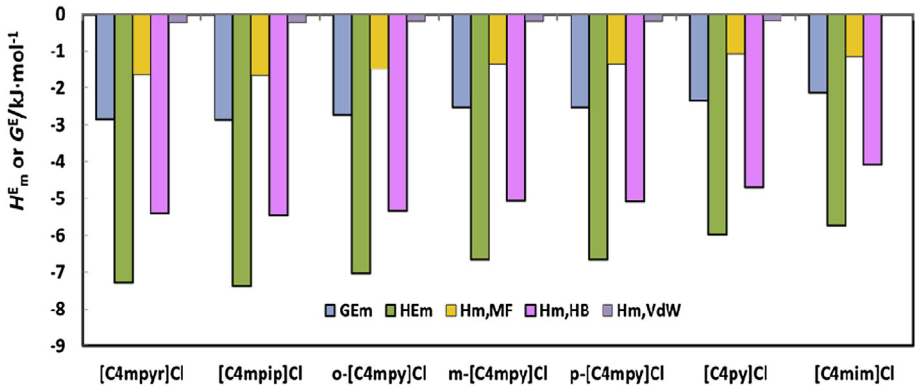

Fig. 4. Excess free Gibbs energy, G^E_m (blue bars) and excess enthalpy, H^E_m (green bars), of (water + pyridinium, pyrrolidinium and piperidinium-based ionic liquids) binary mixture at 298.2 K predicted by COSMO-RS at $x_{H2O} = 0.75$ and contribution of $H^E_{m,MF}$ (orange bars), $H^E_{m,HB}$ (pink bars), and $H^E_{m,vdW}$ (purple bars) to the total excess enthalpy. (For interpretation of the references to color in this figure legend, the reader is referred to the web version of this article.)

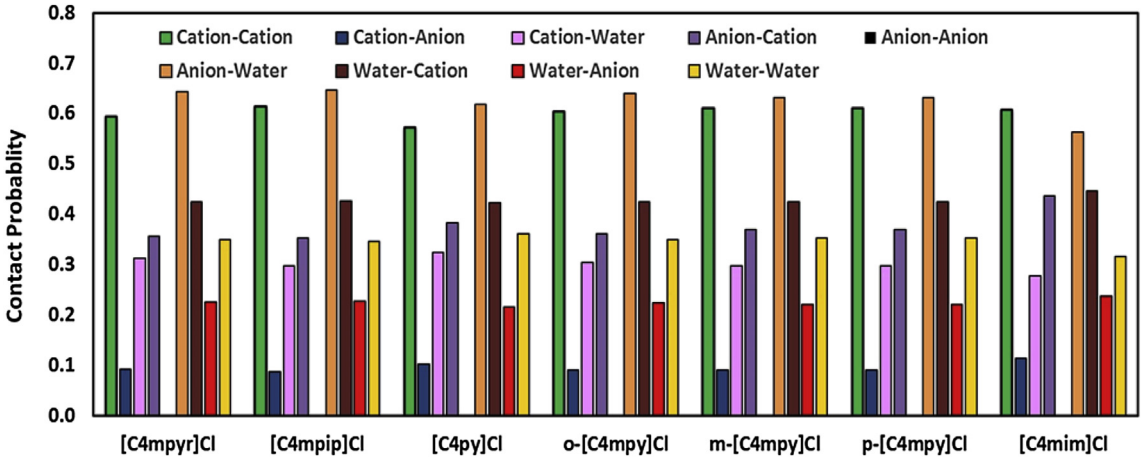

Fig. 5. Contact probability of the binary mixture of ILs and water at 298.2 K using COSMO-RS at $x_{H_2O} = 0.75$ in the term of interaction of Cation–Cation (green bar), Cation–Anion (blue bar), Cation-Water (pink bar), Anion-Cation (purple bar), Anion–Anion (black bar), Anion-Water (orange bar), Water-Cation (brown bar), Water-Anion (red bar), Water–Water (yellow bar). (For interpretation of the references to color in this figure legend, the reader is referred to the web version of this article.)

is that the contact probability for the [Cation]-[Cation] interaction is very significant. Like-charged ions interactions are still a counter-intuitive phenomenon that has been extensively studied by Professor Ralf Ludwig and collaborators at Rostock University [78–80]. According to their findings [Cation]-[Cation] interaction in ILs aqueous systems may appear by substantial charge delocalization in the cation and the use of weakly coordinating anions. This type of phenomenon has been also explained in the literature using both experimental spectroscopic analysis and theoretical DFT calculations [81]. Looking to the contact probability at x_{H_20} ~0.75, it clearly shows that [Anion]-[H_2O] and [Cation]-[Cation] are dominant, showing that the hydrophilicity of the IL is mainly anion dependent, which has been confirmed earlier in the literature by various techniques [48,82], but also indicates that the cation plays an important role [47,82,83].

4. Conclusions

Based on the new experimental water activity data, it was shown that water-ILs interactions are influenced by the aromaticity of cation, the aromatic ILs interacting less with water. COSMO-RS is found to be an excellent tool to interpret the physical-chemistry of water-ILs mixtures, showing high consistency with the experimental measured data. Based on dissociation constants, natural bond orbitals and excess enthalpies it was found that hydrogen bonding is the dominant interaction, most notably between water and the anion, but with a strong influence from the cation–anion interactions. Therefore, to improve the water/ILs interactions, instead of trying to maximize both cation and the anion interactions with water, these results suggest that it should be also taken into consideration the minimization of the cation–anion interactions.

Acknowledgment

This work is being developed in the scope of the projects CICECO-Aveiro Institute of Materials (Ref. FCT UID /CTM /50011/2013), financed by national funds through the FCT/MEC and when applicable co-financed by FEDER under the PT2020 Partnership Agreement, and LSRE/LCM (Ref. FCT UID/EQU/50020/2013). Imran Khan and Mohamed Taha acknowledge Fundação para a Ciência e Tecnologia for the postdoctoral grants SFRH/BPD/76850/2011 and SFRH/BPD/78441/2011, respectively. The authors I. Khan also acknowledges for financial support from FCT for the project EXPL/QEQ-PRS/0224/2013.

Appendix A. Supplementary data

Supplementary data related to this article can be found at http://dx.doi.org/10.1016/j.fluid.2016.01.014.

References

[1] S. Mallakpour, M. Dinari, Ionic liquids as green solvents: progress and prospects, in: A. Mohammad, D. Inamuddin (Eds.), Green Solvents II, Springer, Netherlands, 2012, pp. 1–32.
[2] T. Welton, Ionic liquids in green chemistry, Green Chem. 13 (2011), 225–225.
[3] E. Alvarez-Guerra, A. Irabien, S.P.M. Ventura, J.A.P. Coutinho, Ionic liquid recovery alternatives in ionic liquid-based three-phase partitioning (ILTPP), AlChE J. 60 (2014) 3577–3586.
[4] H. Passos, M.G. Freire, J.A.P. Coutinho, Ionic liquid solutions as extractive solvents for value-added compounds from biomass, Green Chem. 16 (2014) 4786–4815.
[5] H. Passos, I. Khan, F. Mutelet, M.B. Oliveira, P.J. Carvalho, L.M.N.B.F. Santos, C. Held, G. Sadowski, M.G. Freire, J.A.P. Coutinho, Vapor-liquid equilibria of water plus alkylimidazolium-based ionic liquids: measurements and perturbed-chain statistical associating fluid theory modeling, Ind. Eng. Chem. Res. 53 (2014) 3737–3748.
[6] J.F.A. Czajkowska-Żelazko, Applications of Ionic Liquids in Science and Technology, InTech, 2011.
[7] D.R. MacFarlane, N. Tachikawa, M. Forsyth, J.M. Pringle, P.C. Howlett, G.D. Elliott, J.H. Davis, M. Watanabe, P. Simon, C.A. Angell, Energy applications of ionic liquids, Energy Environ. Sci. 7 (2014) 232–250.
[8] J. Pernak, J. Jedraszczyk, J. Krysinski, Effect of New Quaternary Iminium Derivatives Against Selected Bacterium and Fungus Stems, Govi-Verlag, Germany, 1987, 422–422.
[9] J. Pernak, Anticorrosion properties of quaternary ammonium chlorides with alkylthiomethyl radical, Mater. Corros. 35 (1984) 156–159.
[10] M. Sak-Bosnar, Z. Grabaric, B.S. Grabaric, Surfactant sensors in biotechnology part 1-electrochemical sensors, Food Technol. Biotechnol. 42 (2004) 197–206.
[11] E. Grabińska-Sota, J. Kalka, An assessment of the toxicity of pyridinium chlorides and their biodegradation intermediates, Environ. Int. 28 (2003) 687–690.
[12] J.R. Harjani, R.D. Singer, M.T. Garcia, P.J. Scammells, The design and synthesis of biodegradable pyridinium ionic liquids, Green Chem. 10 (2008) 436–438.
[13] S.P.M. Ventura, M. Gurbisz, M. Ghavre, F.M.M. Ferreira, F. Gonçalves, I. Beadham, B. Quilty, J.A.P. Coutinho, N. Gathergood, Imidazolium and pyridinium ionic liquids from mandelic acid derivatives: synthesis and bacteria and algae toxicity evaluation, ACS Sustain. Chem. Eng. 1 (2013) 393–402.
[14] H. Gao, M. Luo, J. Xing, Y. Wu, Y. Li, W. Li, Q. Liu, H. Liu, Desulfurization of fuel by extraction with pyridinium-based ionic liquids, Ind. Eng. Chem. Res. 47 (2008) 8384–8388.
[15] G. Wytze Meindersma, A. Podt, A.B. de Haan, Selection of ionic liquids for the extraction of aromatic hydrocarbons from aromatic/aliphatic mixtures, Fuel Process. Technol. 87 (2005) 59–70.
[16] C.F.C. Marques, T. Mourão, C.M.S.S. Neves, Á.S. Lima, I. Boal-Palheiros, J.A.P. Coutinho, M.G. Freire, Aqueous biphasic systems composed of ionic liquids and sodium carbonate as enhanced routes for the extraction of tetracycline, Biotechnol. Prog. 29 (2013) 645–654.
[17] M. Albrecht, H. Stoeckli-Evans, Catalytically active palladium pyridylidene complexes: pyridinium ionic liquids as n-heterocyclic carbene precursors, Chem. Commun. (2005) 4705–4707.
[18] A.R. Moosavi-Zare, M.A. Zolfigol, M. Zarei, A. Zare, V. Khakyzadeh, Preparation, characterization and application of ionic liquid sulfonic acid functionalized pyridinium chloride as an efficient catalyst for the solvent-free synthesis of 12-aryl-8,9,10,12-tetrahydrobenzo[A]-xanthen-11-ones, J. Mol. Liq. 186 (2013) 63–69.
[19] N.M. Yunus, M.I.A. Mutalib, Z. Man, M.A. Bustam, T. Murugesan, Solubility of CO_2 in pyridinium based ionic liquids, Chem. Eng. J. 189–190 (2012) 94–100.
[20] M.J. Muldoon, S.N.V.K. Aki, J.L. Anderson, J.K. Dixon, J.F. Brennecke, Improving carbon dioxide solubility in ionic liquids, J. Phys. Chem. B 111 (2007) 9001–9009.
[21] J.L. Anderson, J.K. Dixon, J.F. Brennecke, Solubility of CO_2, CH_4, C_2H_6, C_2H_4, O_2, and N_2 in 1-hexyl-3-methylpyridinium bis(trifluoromethylsulfonyl)imide: comparison to other ionic liquids, Acc. Chem. Res. 40 (2007) 1208–1216.
[22] T. Heinze, K. Schwikal, S. Barthel, Ionic liquids as reaction medium in cellulose functionalization, Macromol. Biosci. 5 (2005) 520–525.
[23] E.S. Sashina, D.A. Kashirskii, M. Zaborski, S. Jankowski, Synthesis and dissolving power of 1-alkyl-3-methylpyridinium-based ionic liquids, Russ. J. Gen. Chem. 82 (2012) 1994–1998.
[24] A.B. Pereiro, A. Rodríguez, An ionic liquid proposed as solvent in aromatic hydrocarbon separation by liquid extraction, AlChE J. 56 (2010) 381–386.
[25] A. Westerholt, V. Liebert, J. Gmehling, Influence of ionic liquids on the separation factor of three standard separation problems, Fluid Phase Equilib. 280 (2009) 56–60.
[26] U. Domańska, G.G. Redhi, A. Marciniak, Activity coefficients at infinite dilution measurements for organic solutes and water in the ionic liquid 1-butyl-1-methylpyrrolidinium trifluoromethanesulfonate using GLC, Fluid Phase Equilib. 278 (2009) 97–102.
[27] U. Domańska, M. Królikowski, K. Ślesińska, Phase equilibria study of the binary systems (ionic liquid + thiophene): desulphurization process, J. Chem. Thermodyn. 41 (2009) 1303–1311.
[28] H. Matsumoto, H. Sakaebe, K. Tatsumi, M. Kikuta, E. Ishiko, M. Kono, Fast cycling of Li/$LiCoO_2$ cell with low-viscosity ionic liquids based on bis(-fluorosulfonyl)imide $[FSI]^-$, J. Power Sources 160 (2006) 1308–1313.
[29] J. Jin, H.H. Li, J.P. Wei, X.K. Bian, Z. Zhou, J. Yan, Li/$LiFePO_4$ batteries with room temperature ionic liquid as electrolyte, Electrochem. Commun. 11 (2009) 1500–1503.
[30] A.-L. Pont, R. Marcilla, I. De Meatza, H. Grande, D. Mecerreyes, Pyrrolidinium-based polymeric ionic liquids as mechanically and electrochemically stable polymer electrolytes, J. Power Sources 188 (2009) 558–563.
[31] H. Sakaebe, H. Matsumoto, N-methyl-N-propylpiperidinium bis(trifluoromethanesulfonyl)imide (PP13–TFSI) – Novel electrolyte base for Li battery, Electrochem. Commun. 5 (2003) 594–598.
[32] M. Shukla, S. Saha, A Comparative Study of Piperidinium and Imidazolium Based Ionic Liquids: Thermal, Spectroscopic and Theoretical Studies, 2013.
[33] J. Neumann, S. Steudte, C.-W. Cho, J. Thoming, S. Stolte, Biodegradability of 27 pyrrolidinium, morpholinium, piperidinium, imidazolium and pyridinium ionic liquid cations under aerobic conditions, Green Chem. 16 (2014) 2174–2184.
[34] M. Blahušiak, Š. Schlosser, Physical properties of phosphonium ionic liquid and its mixtures with dodecane and water, J. Chem. Thermodyn. 72 (2014) 54–64.
[35] H.F.D. Almeida, J.A. Lopes-da-Silva, M.G. Freire, J.A.P. Coutinho, Surface tension and refractive index of pure and water-saturated tetradecyltrihexylphosphonium-based ionic liquids, J. Chem. Thermodyn. 57 (2013) 372–379.
[36] J.A. Widegren, E.M. Saurer, K.N. Marsh, J.W. Magee, Electrolytic conductivity of four imidazolium-based room-temperature ionic liquids and the effect of a water impurity, J. Chem. Thermodyn. 37 (2005) 569–575.
[37] B.D. Fitchett, T.N. Knepp, J.C. Conboy, 1-Alkyl-3-methylimidazolium bis(perfluoroalkylsulfonyl)imide water-immiscible ionic liquids: the effect of water on electrochemical and physical properties, J. Electrochem. Soc. 151 (2004) E219–E225.
[38] N. Yaghini, L. Nordstierna, A. Martinelli, Effect of water on the transport properties of protic and aprotic imidazolium ionic liquids – An analysis of self-diffusivity, conductivity, and proton exchange mechanism, Phys. Chem. Chem. Phys. 16 (2014) 9266–9275.
[39] R.A. Brown, P. Pollet, E. McKoon, C.A. Eckert, C.L. Liotta, P.G. Jessop, Asymmetric hydrogenation and catalyst recycling using ionic liquid and supercritical carbon dioxide, J. Am. Chem. Soc. 123 (2001) 1254–1255.
[40] S. Keskin, D. Kayrak-Talay, U. Akman, O. Hortacsu, A review of ionic liquids towards supercritical fluid applications, J. Supercrit. Fluids 43 (2007) 150–180.
[41] D. Chakrabarty, A. Chakraborty, D. Seth, N. Sarkar, Effect of water, methanol, and acetonitrile on solvent relaxation and rotational relaxation of Coumarin 153 in neat 1-hexyl-3-methylimidazolium hexafluorophosphate, J. Phys. Chem. A 109 (2005) 1764–1769.
[42] V. Najdanovic-Visak, L.P.N. Rebelo, M. Nunes da Ponte, Liquid-liquid behaviour of ionic liquid-1-butanol-water and high pressure CO_2-induced phase changes, Green Chem. 7 (2005) 443–450.
[43] M. Anouti, J. Jones, A. Boisset, J. Jacquemin, M. Caillon-Caravanier, D. Lemordant, Aggregation behavior in water of new imidazolium and pyrrolidinium alkycarboxylates protic ionic liquids, J. Colloid Interface Sci. 340 (2009) 104–111.
[44] M. Anouti, A. Vigeant, J. Jacquemin, C. Brigouleix, D. Lemordant, Volumetric Properties, viscosity and refractive index of the protic ionic liquid, pyrrolidinium octanoate, in molecular solvents, J. Chem. Thermodyn. 42 (2010) 834–845.
[45] K. Paduszyński, U. Domańska, Experimental and theoretical study on infinite dilution activity coefficients of various solutes in piperidinium ionic liquids, J. Chem. Thermodyn. 60 (2013) 169–178.
[46] A.A. Niazi, B.D. Rabideau, A.E. Ismail, Effects of water concentration on the structural and diffusion properties of imidazolium-based ionic liquid–water mixtures, J. Phys. Chem. B 117 (2013) 1378–1388.
[47] I. Khan, M. Taha, P. Ribeiro-Claro, S.P. Pinho, J.A.P. Coutinho, Effect of the cation on the interactions between alkyl methyl imidazolium chloride ionic liquids and water, J. Phys. Chem. B 118 (2014) 10503–10514.
[48] I. Khan, K.A. Kurnia, F. Mutelet, S.P. Pinho, J.A. Coutinho, Probing the interactions between ionic liquids and water: experimental and quantum chemical approach, J. Phys. Chem. B 118 (2014) 1848–1860.
[49] A. Bhattacharjee, P.J. Carvalho, J.A.P. Coutinho, The effect of the cation aromaticity upon the thermophysical properties of piperidinium- and pyridinium-based ionic liquids, Fluid Phase Equilib. 375 (2014) 80–88.
[50] M.B. Oliveira, F. Llovell, J.A.P. Coutinho, L.F. Vega, Modeling the [NTf2] pyridinium ionic liquids family and their mixtures with the soft statistical associating fluid theory equation of state, J. Phys. Chem. B 116 (2012) 9089–9100.
[51] M.G. Freire, C.M.S.S. Neves, K. Shimizu, C.E.S. Bernardes, I.M. Marrucho, J.A.P. Coutinho, J.N.C. Lopes, L.P.N. Rebelo, Mutual solubility of water and structural/positional isomers of n-alkylpyridinium-based ionic liquids, J. Phys. Chem. B 114 (2010) 15925–15934.
[52] T. Singh, A. Kumar, Cation–anion–water interactions in aqueous mixtures of imidazolium based ionic liquids, Vib. Spectrosc. 55 (2011) 119–125.
[53] I. López-Martin, E. Burello, P.N. Davey, K.R. Seddon, G. Rothenberg, Anion and cation effects on imidazolium salt melting points: a descriptor modelling study, ChemPhysChem 8 (2007) 690–695.
[54] M.G. Freire, L.M.N.B.F. Santos, A.M. Fernandes, J.A.P. Coutinho, I.M. Marrucho, An overview of the mutual solubilities of water–imidazolium-based ionic liquids systems, Fluid Phase Equilib. 261 (2007) 449–454.
[55] L. Crowhurst, P.R. Mawdsley, J.M. Perez-Arlandis, P.A. Salter, T. Welton, Solvent-solute interactions in ionic liquids, Phys. Chem. Chem. Phys. 5 (2003)

2790–2794.
[56] A. Klamt, COSMO-RS from Quantum Chemistry to Fluid Phase Thermodynamics and Drug Design, Elsevier, Amsterdam, The Netherlands, 2005.
[57] A. Klamt, The COSMO and COSMO-RS solvation models, Wires Comput. Mol. Sci. 1 (2011) 699–709.
[58] G. Vakili-Nezhaad, M. Vatani, M. Asghari, Calculation of the binary interaction and nonrandomness parameters of NRTL, NRTL1, AND NRTL2 models using genetic algorithm for ternary ionic liquid systems, Chem. Eng. Commun. 200 (2013) 1102–1120.
[59] S. Martinho, J.M.M. Araújo, L.P.N. Rebelo, A.B. Pereiro, I.M. Marrucho, (Liquid + liquid) equilibria of perfluorocarbons with fluorinated ionic liquids, J. Chem. Thermodyn. 64 (2013) 71–79.
[60] I. Khan, M.L. Batista, P.J. Carvalho, L.M. Santos, J.R. Gomes, J.A. Coutinho, Vapor-liquid equilibria of imidazolium ionic liquids with cyano containing anions with water and ethanol, J. Phys. Chem. B 119 (2015) 10287–10303.
[61] W.J. Hamer, Y.C. Wu, Osmotic coefficients and mean activity coefficients of uni-univalent electrolytes in water at 25° C, J. Phys. Chem. Ref. Data 1 (1972) 1047–1100.
[62] A. Klamt, F. Eckert, COSMO-RS: a novel and efficient method for the a priori prediction of thermophysical data of liquids, Fluid Phase Equilib. 172 (2000) 43–72.
[63] A. Klamt, Conductor-like screening model for real solvents: a new approach to the quantitative calculation of solvation phenomena, J. Phys. Chem. 99 (1995) 2224–2235.
[64] M. Diedenhofen, F. Eckert, A. Klamt, Prediction of infinite dilution activity coefficients of organic compounds in ionic liquids using COSMO-RS, J. Chem. Eng. Data 48 (2003) 475–479.
[65] R. Putnam, R. Taylor, A. Klamt, F. Eckert, M. Schiller, Prediction of infinite dilution activity coefficients using COSMO-RS, Ind. Eng. Chem. Res. 42 (2003) 3635–3641.
[66] K.A. Kurnia, J.A.P. Coutinho, Overview of the excess enthalpies of the binary mixtures composed of molecular solvents and ionic liquids and their modeling using COSMO-RS, Ind. Eng. Chem. Res. 52 (2013) 13862–13874.
[67] A.K.F. Eckert, COSMOtherm Version C2.1 Release 01.08, COSMOlogic GmbH & Co. KG, Leverkusen, Germany, 2006.
[68] J.G. Huddleston, R.D. Rogers, Room temperature ionic liquids as novel media for 'clean' liquid-liquid extraction, Chem. Commun. (1998) 1765–1766.
[69] P. Bonhôte, A.-P. Dias, N. Papageorgiou, K. Kalyanasundaram, M. Grätzel, Hydrophobic, highly conductive ambient-temperature molten salts†, Inorg. Chem. 35 (1996) 1168–1178.
[70] P.A.Z. Suarez, S. Einloft, J.E.L. Dullius, R.F. de Souza, J. Dupont, Synthesis and physical-chemical properties of ionic liquids based on 1-n-butyl-3-methylimidazolium cation, J. Chim. Phys. 95 (1998) 1626–1639.
[71] N.N. Wang, Q.G. Zhang, F.G. Wu, Q.Z. Li, Z.W. Yu, Hydrogen bonding interactions between a representative pyridinium-based ionic liquid BuPy BF_4 and water/dimethyl sulfoxide, J. Phys. Chem. B 114 (2010) 8689–8700.
[72] I. Khan, K.A. Kurnia, T.E. Sintra, J.A. Saraiva, S.P. Pinho, J.A.P. Coutinho, Assessing the activity coefficients of water in cholinium-based ionic liquids: experimental measurements and COSMO-RS modeling, Fluid Phase Equilib. 361 (2014) 16–22.
[73] M.J. Frisch, G.W. Trucks, H.B. Schlegel, G.E. Scuseria, M.A. Robb, J.R. Cheeseman, G. Scalmani, V. Barone, et al., Gaussian 09, Gaussian, Inc., Wallingford, CT, USA, 2009.
[74] K.A. Kurnia, S.P. Pinho, J.A.P. Coutinho, Designing ionic liquids for absorptive cooling, Green Chem. 16 (2014) 3741–3745.
[75] C.G. Hanke, R.M. Lynden-Bell, A simulation study of water–dialkylimidazolium ionic liquid mixtures, J. Phys. Chem. B 107 (2003) 10873–10878.
[76] V. Migliorati, A. Zitolo, P. D'Angelo, Using a combined theoretical and experimental approach to understand the structure and dynamics of imidazolium-based ionic liquids/water mixtures. 1. Md simulations, J. Phys. Chem. B 117 (2013) 12505–12515.
[77] S. Tsuzuki, H. Tokuda, M. Mikami, Theoretical analysis of the hydrogen bond of imidazolium C_2-H with anions, Phys. Chem. Chem. Phys. 9 (2007) 4780–4784.
[78] K. Fumino, K. Wittler, R. Ludwig, The anion dependence of the interaction strength between ions in imidazolium-based ionic liquids probed by far-infrared spectroscopy, J. Phys. Chem. B 116 (2012) 9507–9511.
[79] K. Fumino, T. Peppel, M. Geppert-Rybczynska, D.H. Zaitsau, J.K. Lehmann, S.P. Verevkin, M. Kockerling, R. Ludwig, The influence of hydrogen bonding on the physical properties of ionic liquids, Phys. Chem. Chem. Phys. 13 (2011) 14064–14075.
[80] R. Ludwig, A. Knorr, K. Fumino, F.A. Weinhold, Spectroscopic evidence for clusters of like-charged ions in ionic liquids stabilized by cooperative hydrogen bonding. Chem. Phys. Chem. DOI: 10.1002/cphc.201501134.
[81] A. Mele, C.D. Tran, S.H. De Paoli Lacerda, The structure of a room-temperature ionic liquid with and without trace amounts of water: the role of C-H···O and C-H···F interactions in 1-n-butyl-3-methylimidazolium tetrafluoroborate, Angew. Chem. Int. Ed. 42 (2003) 4364–4366.
[82] L. Cammarata, S.G. Kazarian, P.A. Salter, T. Welton, Molecular states of water in room temperature ionic liquids, Phys. Chem. Chem. Phys. 3 (2001) 5192–5200.
[83] T. Masaki, K. Nishikawa, H. Shirota, Microscopic study of ionic liquid–H_2O systems: alkyl-group dependence of 1-alkyl-3-methylimidazolium cation, J. Phys. Chem. B 114 (2010) 6323–6331.